

# Effects of PCB Substrate Surface Finish and Flux on Solderability of Lead-Free SAC305 Alloy

A. Siewiorek, A. Kudyba, N. Sobczak, M. Homa, Z. Huber, Z. Adamek, and J. Wojewoda-Budka

(Submitted November 20, 2012; published online February 15, 2013)

The solderability of the SAC305 alloy in contact with printed circuit boards (PCB) having different surface finishes was examined using the wetting balance method. The study was performed at a temperature of 260 °C on three types of PCBs covered with (1) hot air solder leveling (HASL LF), (2) electroless nickel immersion gold (ENIG), and (3) organic surface protectant (OSP), organic finish, all on Cu substrates and two types of fluxes (EF2202 and RF800). The results showed that the PCB substrate surface finish has a strong effect on the value of both the wetting time  $t_0$  and the contact angle  $\theta$ . The shortest wetting time was noted for the OSP finish ( $t_0 = 0.6$  s with EF2202 flux and  $t_0 = 0.98$  s with RF800 flux), while the ENIG finish showed the longest wetting time ( $t_0 = 1.36$  s with EF2202 flux and  $t_0 = 1.55$  s with RF800 flux). The  $\theta$  values calculated from the wetting balance tests were as follows: the lowest  $\theta$  of 45° was formed on HASL LF (EF2202 flux), the highest  $\theta$  of 63° was noted on the OSP finish, while on the ENIG finish, it was 58° (EF2202 flux). After the solderability tests, the interface characterization of cross-sectional samples was performed by means of scanning electron microscopy coupled with energy dispersive spectroscopy.

**Keywords** flux, lead-free SAC305 alloy, PCB finish, solderability, wetting balance test

## 1. Introduction

The SAC305 (SnAg3.0Cu0.5, wt.%) alloy belongs to the SAC family of Pb-free solders recommended for the joining of various components in electronic devices, particularly in printed circuit boards (PCB). SAC alloys, compared with traditional Sn-Pb eutectic solders, have a higher melting temperature and better mechanical properties, enhanced strength, improved creep, and thermal fatigue characteristics (Ref 1-6). However, following the literature data, the implementation of SAC alloys on an industrial scale is accompanied by some problems such as the formation of brittle intermetallic compounds (IMCs), short creep-rupture lifetime (Ref 1, 2), insufficient wetting (Ref 7, 8), unsatisfactory solderability, and thus low reliability, compared to conventional Sn-Pb solders.

It is well known that among different possible solutions, the solderability improvement can be achieved by appropriate selection of fluxes (Ref 9-13). In such a case, the flux selected should provide not only the effective protection of the surfaces of both a solder and a material to be joined from oxidation during soldering but also should assure the effective removal of

the primary oxide films always present on these surfaces (Ref 14, 15).

Another important factor affecting reliability of solder joints in electronic devices is the PCB surface finish since it forms a critical interface between the bare PCB and the component to be assembled. The family of functional coatings of solder mask over bare copper (SMOBC) type is commonly used in practice as a PCB surface finish, which has two main functions, i.e., to protect the exposed copper circuitry and to provide a solderable surface when assembling (soldering) the components to the board. Among different SMOBC finishes throughout the printed circuit industry, there are three types most used in practice:

- (1) Hot air solder leveling (HASL LF) process used for deposition of lead-free solder coating on Cu substrate. The typical thickness of HASL LF is 1.3-35  $\mu\text{m}$ . The benefits of this kind of PBS finish are low cost coupled with good shelf life and excellent solderability, while its disadvantages are non-uniformity of the coating, low thermal shock resistance, and the formation of brittle IMCs at the interface during both processing and solder joints' operation.
- (2) Electroless nickel immersion gold (ENIG) coating deposited on Cu substrate. It is composed of two layers, i.e., a gold layer of a typical thickness of 0.05-0.25  $\mu\text{m}$  over nickel containing a phosphorous layer of 1-8  $\mu\text{m}$  thickness. The main advantages of this PCB finish are long-term experience and good knowledge of the product behavior under different conditions, its excellent corrosion resistance, solderability, and shelf life (1 year). However, ENIG has higher production cost and this is the only PCB finish that requires a two-stage process. Moreover, the uncontrolled quality of that kind of finish may decrease the solder joint reliability due to the appearance of such structural defects as a "Black Pad."
- (3) Organic surface protectant (OSP) on Cu substrate. Its typical thickness is 0.2-0.5  $\mu\text{m}$ . More recent OSP

A. Siewiorek, A. Kudyba, N. Sobczak, and M. Homa, Centre for High-Temperature Studies, Foundry Research Institute, 73 Zakopianska St., 30-418 Cracow, Poland; Z. Huber and Z. Adamek, Fideltronik IMEL Ltd, 1 Beniowskiego St., 34-200 Sucha Beskidzka, Poland; and J. Wojewoda-Budka, Institute of Metallurgy and Materials Science, Polish Academy of Sciences, 25 Reymonta St., 30-059 Cracow, Poland. Contact e-mails: aleksandra.siewiorek@gmail.com and asiewior@iod.krakow.pl.

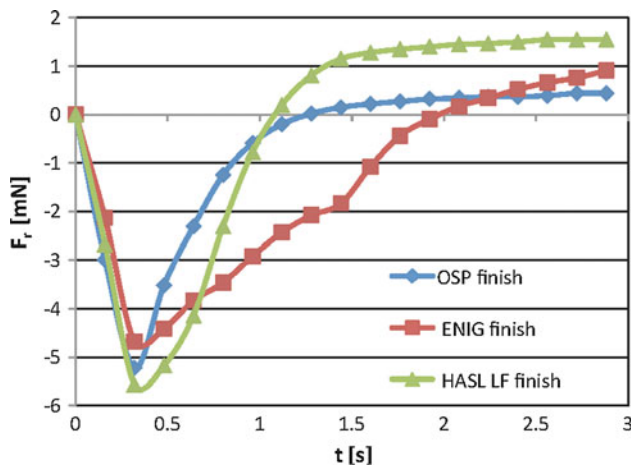


**Fig. 1** Effect of surface finish on wetting behavior of SAC305 (260 °C, 3 s) with RF800 flux

formulas are designed for lead-free assembly and they can handle multiple heat cycles and have a 1-year shelf life. However, difficult or impossible inspection of the final product is the main disadvantage of the OSP finish.

In the present work, the influence of the type of flux and PCB surface finish (HASL LF, ENIG, OSP) on the solderability of SAC305 alloy with selected PCBs was investigated. It was accomplished using the wetting balance method, which allows the direct measurements of the wetting force and wetting time and indirect determination of the contact angle values (Ref 16 - 18).

## 2. Materials and Testing

In order to reproduce as closely as possible the technological conditions of soldering in practice, the commercial Pb-free SAC305 solder (3.1Ag, 0.8Cu, 0.04Pb, wt.%) was applied.

The solderability of SAC305 alloy was examined by the wetting balance method on the MENISCO ST88 (Metronlec, France) apparatus using the same procedure and under the same conditions as in the industrial wave soldering process (Ref 19), i.e., at a temperature of 260 °C for 3-s contact in air with a flux.

Three types of PCBs, i.e., glass-epoxy laminates with the following surface finishes, were used: (1) HASL LF (lead-free); (2) ENIG—composed of Ni-P layer (with 4-6 μm thickness) and Au layer (0.1 μm thickness); and (3) OSP.

The test samples taken from the PCB were in the form of a coupon of 4.5 mm length, 3.4 mm width, and 1.6 mm thickness with two flat long surfaces. Two kinds of commercial fluxes EF2202 and RF800 were used.

EF2202 is a VOC-free, halide-free, rosin/resin-free, low solid no-clean flux which provides the highest activity of any VOC-free Bellcore compliant flux for defect-free soldering. It is formulated with a proprietary mixture of organic activators, which deliver excellent wetting and top-side hole fill, even with OSP-coated bare copper boards having undergone prior thermal excursions.

RF800 provides the broadest process window for a no-clean flux with less than 5% solid content. RF800 is designed to provide excellent soldering results (low defects rates), even

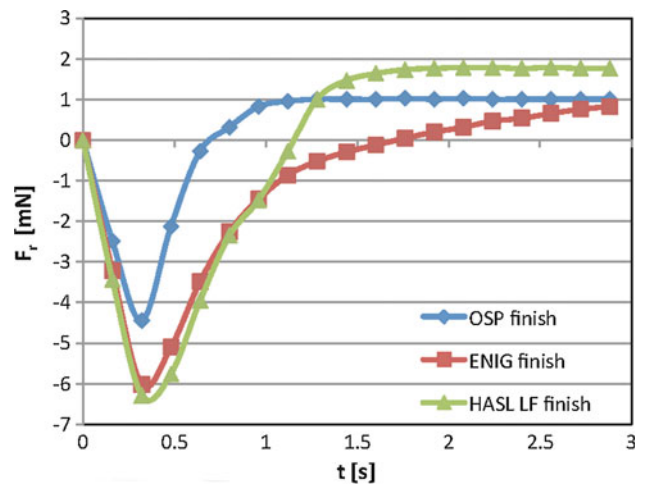


**Fig. 2** Effect of surface finish on wetting behavior of SAC305 (260 °C, 3 s) with EF2202 flux

when the surfaces to be soldered (component leads and pads) are not highly solderable. RF800 works particularly well with bare copper boards protected with organic or rosin/resin coatings and with tin-lead-coated PCBs (<http://alphacpmd.com/Products/Liquid-Soldering-Flux/RF-800>).

Just before the wetting balance tests, each coupon was dipped into the flux. Excessive flux was removed by touching the end of the coupon by filter paper and then the sample was immersed into a bath of molten SAC305 solder. The immersion depth and the immersion-withdrawing speed were 1 mm and 20 mm/s, respectively. For each condition, five tests were made. During the tests, the wetting curves were automatically recorded (force  $F_r$  as a function of time  $t$ ).

After wetting balance tests, the cross sections of the examined samples were prepared using standard metallographic procedures. The interface characterization of the produced alloy/substrate couples was made using a ZEISS Axio light microscope (LM). The microstructural observations were performed in bright field (BF) and in differential interference contrast (DIC) under magnifications of 50-1500×. Additionally, the scanning electron microscopy (SEM) observations coupled with an energy dispersive x-ray spectroscopy (EDS) analysis of interfaces formed in solder/substrate couples were made using FEI Quanta 3D FEG microscope equipped with EDAX GENESIS 4000 spectrometer.

## 3. Results and Discussion

Typical acquired wetting balance curves that represent the change of measured force ( $F_r$ ) versus time ( $t$ ) and characterize the dynamic wetting behavior of the SAC305 solder on PCB substrates with different surface finishes are shown in Fig. 1 and 2 for RF800 and EF2202 flux, respectively. The results obtained from wetting balance tests are summarized in Fig. 3, where Fig. 3(a) presents the data obtained at the maximum value of force  $F_r$  (resultant force measured by the balance):

$$F_r = F_w - F_a \quad (\text{Eq 1})$$

This static force was achieved after specified time when an equilibrium state during wetting tests was reached. In Fig. 3(b), one may compare the values of wetting time  $t_0$ , where  $t_0$

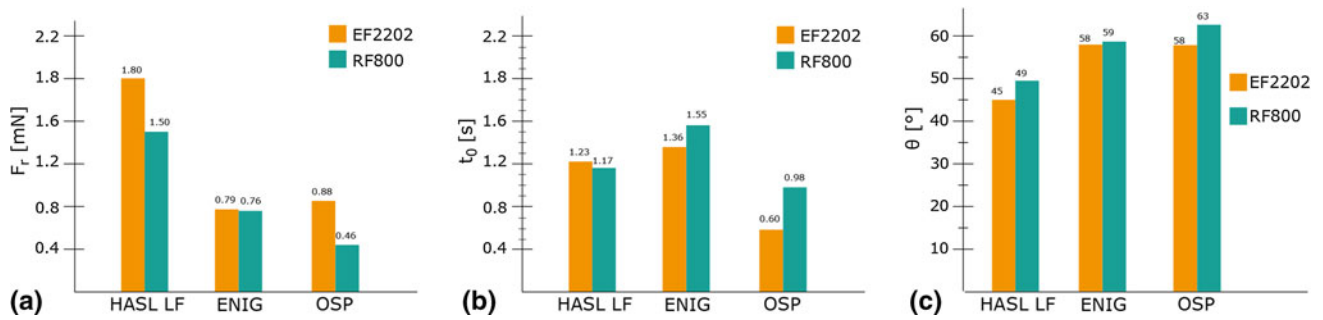


**Fig. 3** Comparison of the effect of surface finish type and flux type on the values of recorded force  $F_r$  (a), wetting time  $t_0$  (b), and contact angle  $\theta$  (c) in SAC305/substrate couples (260 °C, 3 s)

**Table 1** Contact angles formed with SAC305 solder on different PCB surface finishes (260°, 3 s)

Surface finish type Flux type	HASL LF lead-free		ENIG		OSP	
	EF 2202	RF 800	EF 2202	RF 800	EF 2202	RF 800
Contact angle value						
Test 1	46°	49°	58°	57°	61°	67°
Test 2	42°	52°	59°	59°	56°	63°
Test 3	46°	49°	59°	57°	58°	61°
Test 4	46°	49°	55°	60°	56°	56°
Test 5	45°	47°	60°	61°	59°	70°
Average value	45°	49°	58°	59°	58°	63°

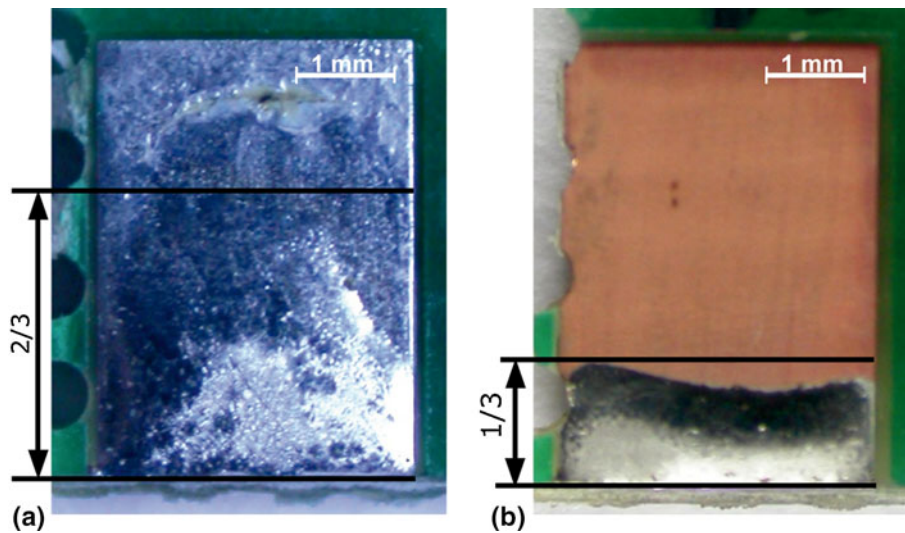


**Fig. 4** Side view of SAC305/substrate samples after wetting balance tests (260 °C, 3 s) with RF800 flux: HASL LF (a); OSP (b)

denotes the moment when the wetting force  $F_w$  is equal to buoyancy force ( $F_a$ —Archimedeian push) and at that time, the measured wetting force is zero. Knowing  $F_r$ , we can extract the wetting force  $F_w$  from the measurement by adding the Archimedeian push  $F_a$ :

$$F_a = \rho * v * g \quad (\text{Eq 2})$$

$$F_w = \gamma_{LV} * l * \cos \theta \quad (\text{Eq 3})$$

$$\gamma_{LV} * l * \cos \theta = F_r + \rho * v * g \quad (\text{Eq 4})$$

The obtained results show that the shortest wetting time  $t_0$  was noted for the OSP finish ( $t_0 = 0.6$  s with EF2202 flux and  $t_0 = 0.98$  s with RF800 flux), while the longest one was in the case of the ENIG finish ( $t_0 = 1.36$  s with EF2202 flux and  $t_0 = 1.55$  s with FR800 flux) (Fig. 1, 2). In the case of the HASL LF finish, the wetting time reached the value of  $t_0 = 1.23$  s with EF2202 flux and  $t_0 = 1.17$  s with RF800 flux. The buoyancy force  $F_a$  has the value of  $F_a = -0.93$  mN.

The measured force  $F_r$  of SAC305 with the HASL LF finish using RF800 flux (Fig. 1) was larger ( $F_r = 1.50$  mN) than those

obtained for the OSP ( $F_r = 0.46$  mN) and ENIG ( $F_r = 0.76$  mN) ones. With EF2202 flux (Fig. 2), the largest value of the recorded force  $F_r$  was obtained also for the HASL LF finish ( $F_r = 1.80$  mN).

According to Fig. 3(a) and (b), the OSP finish with both fluxes shows the smallest values of the recorded force ( $F_r = 0.52$  mN with RF800 flux and  $F_r = 1.03$  mN with EF2202 flux) as well as the wetting time  $t_0 = 0.98$  s with RF800 flux and  $t_0 = 0.6$  s with EF2202 flux.

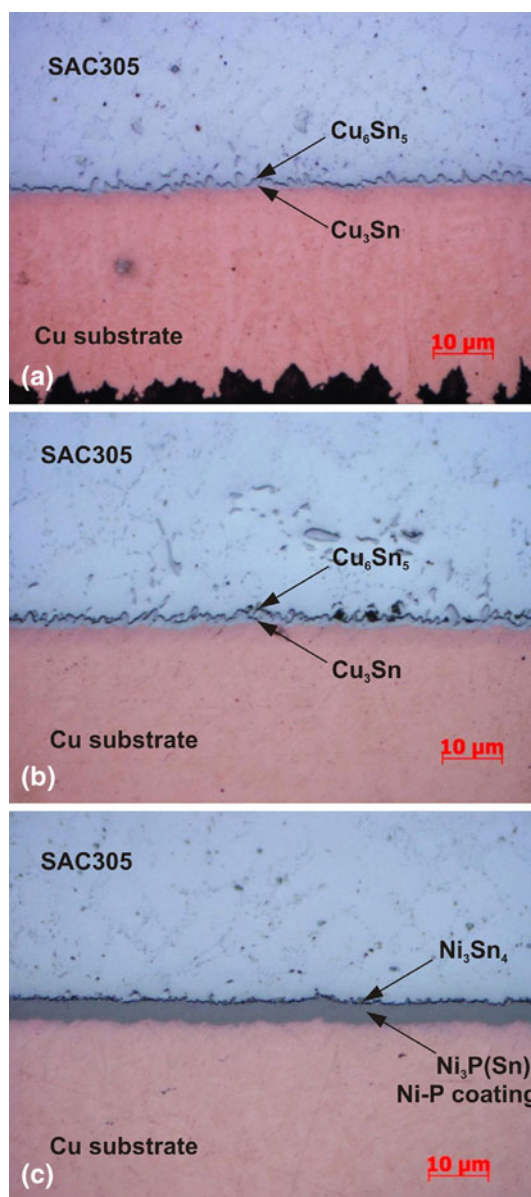
The contact angle values  $\theta$  for examined combinations of materials in solderability tests are shown in Fig. 3(c) and are collected in Table 1. The final contact angle values were calculated on the basis of the data recorded in the wetting balance tests using software supplied with the Menisco ST88 apparatus. The value  $\theta$  is representative of the wetting quality and it characterizes the solderability of the materials. The smaller the  $\theta$ , the better both wettability and solderability. The lowest value of the contact angle for SAC305 is observed on the HASL LF finish ( $\theta = 45^\circ$ ), while the highest one is formed on the OSP type ( $\theta = 63^\circ$ ). No significant difference in the wetting behavior and contact angles was noted between the selected three fluxes.

Solderability quality is classified into four classes as follows (Ref 18, 20):

- Class 1:* excellent quality, contact angle 0-30°;
- Class 2:* good quality, contact angle 31-40°;
- Class 3:* admissible quality, contact angle 41-55°;
- Class 4:* uncertain quality, contact angle 56-70°.

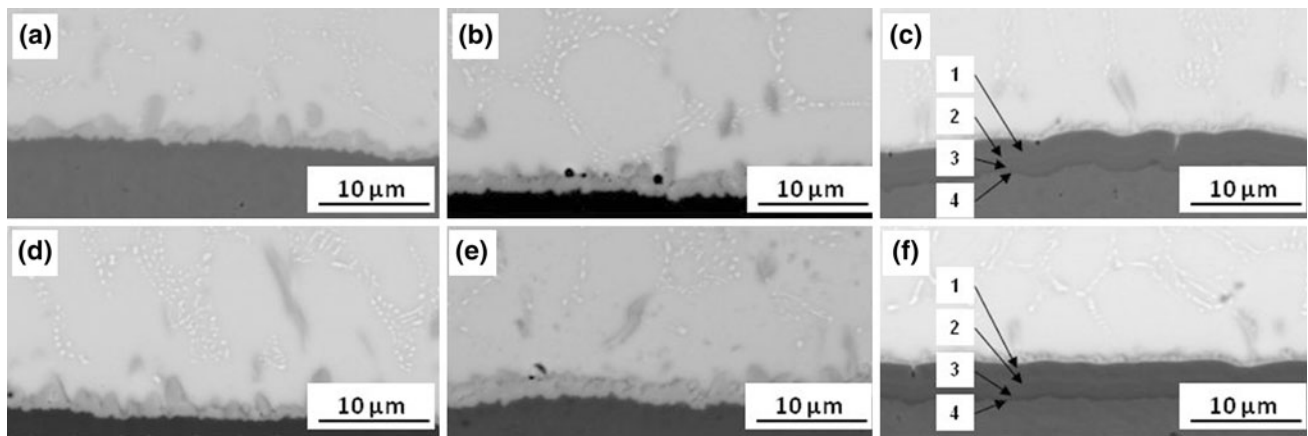
The results of wetting balance tests show good agreement with visual observation of the degree of solder spreading over the PCB surface finishes. For the HASL LF finish and RF800 flux (Fig. 4a), the solder covers 2/3 of the test coupon surface with a corresponding contact angle  $\theta$  of 45° and solderability class 3. In the case of the OSP finish and RF800 flux, the solder covers a much smaller area of only 1/4-1/3 of the surface (Fig. 4b), and it forms the higher contact angle value of 63° that corresponds to the solderability class 4.

Figure 5 shows the LM-DIC images of the microstructure of the cross-sectioned samples after wetting balance tests. During the 3-s immersion time, molten SAC305 solder reacts with the substrate to form the interfaces of complex structures. Their SEM/EDX observations confirmed the formation of the continuous IMC at the substrate/solder interface. Figure 6 presents the comparison of the microstructure of this interfacial region for all the types of finishes, each represented by two pictures. It could be easily noticed that the IMC shows typical scallop-shaped morphology. Its thickness is very similar for the OSP and HASL LF finishes, which is about 2  $\mu\text{m}$  (Fig. 6a, b, d, e), while for ENIG, the IMC layer is thinner ( $\sim 0.5$   $\mu\text{m}$ ). Typically, for wave soldering process, such thin intermetallic layers are observed in the case of SnPb solder, while for lead-free ones, they are twice thicker. Spalling of the IMC was mostly observed in the case of the HASL LF finish (Fig. 6b, e), regardless of the flux type used. On the other hand, the EDX microchemical analysis showed that for both HASL LF and OSP finishes, the intermetallic layer at the solder/side interface is the  $\text{Cu}_6\text{Sn}_5$  phase. Conversely, for the ENIG finish, the chemical composition of the IMC layer (6.7Ag, 54.5Sn, 20.0Ni, and 18.8Cu, at.%) corresponds to the  $(\text{Ni,Cu})_3\text{Sn}_4$  phase. This phase was deduced taking into account three facts: (1) the tin amount corresponds to the  $\text{Ni}_3\text{Sn}_4$  phase, (2) no



**Fig. 5** Cross-sectional images of SAC305/substrate samples after wetting balance test (260 °C, 3 s): OSP with RF800 flux (a), HASL LF with EF2202 flux (b), and ENIG with RF800 flux (c)

excess of copper, which could indicate the formation of  $\text{Cu}_6\text{Sn}_5$ , is detected, and (3) the IMC layer is very thin and therefore information on local chemical composition obtained by EDS analysis also comes from the matrix due to the beam broadening. This result confirms the validity of the thesis that among the two most popular intermetallics,  $\text{Ni}_3\text{Sn}_4$  and  $\text{Cu}_6\text{Sn}_5$ , the first one should be formed primarily if the copper content is below 0.6 wt.%, which corresponds to 1.11 at.% (Ref 21). Moreover, only in the case of the ENIG finish, the enrichment in silver (up to 8.6 at.%) within  $(\text{Ni,Cu})_3\text{Sn}_4$  was observed. According to previous studies (Ref 22), such enrichment was noted for the  $\text{Cu}_6\text{Sn}_5$  phase where the absorption of fine  $\text{Ag}_3\text{Sn}$  particles on the IMC surface took place, particularly for the scallops of  $\text{Cu}_6\text{Sn}_5$  formed by the ripening because the  $\text{Ag}_3\text{Sn}$  nanoparticles decrease the surface energy and hinder the growth of the  $\text{Cu}_6\text{Sn}_5$  phase.



**Fig. 6** SEM micrographs of SAC305/substrate samples after wetting balance test (260 °C, 3 s) with different fluxes: OSP&EF2202 flux (a), HASL&EF2202 flux (b), ENIG&EF2202 flux (c), OSP&RF800 flux (d), HASL&RF800 flux (e), and ENIG&RF800 flux (f)

During soldering with the ENIG finish, the original Ni-P plating transformed into a multilayer region where four layers can be distinguished (Fig. 6c, f). Two of them characterized by the largest thickness were of similar contrast and composition. The upper layer next to the IMC (marked with No. 1) was composed of 18.8-19.3 P, 1.3-1.5 Sn, and 79.2-80 Ni (at.%), while the bottom one (marked by No. 3 in Fig. 6c, f) contained 31.3 P and 68.7 Ni (at.%). Two other layers (No. 2 and No. 4 in Fig. 6c, f, respectively) were too thin for EDS measurements as in their case, the beam broadening and escape depth for x-rays hinder the analysis of the individual layer. Following the literature data, during processing, the Ni-P amorphous plating transforms into a layer containing 17.1 at.% P and 82.9 at.% Ni and a P-rich layer containing 28 at.% P and 72 at.% Ni, which is identified mostly as  $Ni_3P$  or  $Ni_{12}P_5$  phase, respectively (Ref 23, 24).

## 4. Conclusions

The wetting balance measurements of solderability of the SAC305 alloy in contact with PCB having three different surface finishes (HASL LF, ENIG, and OSP) on Cu substrates and using two types of fluxes (EF2202 and RF800) are evidenced as follows:

- (1) The type of surface finish has a strong effect on the solderability with SAC305, measured in terms of both wetting force  $F_r$  and wetting time  $t_0$ .
- (2) The highest values of  $F_r$  were recorded for the HASL LF finish with EF2202 flux ( $F_r = 1.80$  mN) and with RF800 flux ( $F_r = 1.50$  mN), while the lowest ones were for the OSP finish with EF2202 flux ( $F_r = 0.88$  mN) and RF800 flux ( $F_r = 0.46$  mN).
- (3) The flux affects the wetting time  $t_0$ , especially on the ENIG and OSP finishes. The shortest wetting time of 0.6-0.98 s was noted with the OSP finish, while the ENIG finish showed the longest wetting time of 1.36-1.55 s.
- (4) The contact angle values were comparable for both types of fluxes for all examined types of finishes. The highest contact angle was noted for the OSP finish showing  $63^\circ$  with RF800 flux and  $58^\circ$  with EF2202 flux.

- (5) Under conditions of this study, the admissible solder quality (solderability class 3) was obtained only for the HASL LF finish, while the OSP and ENIG finishes have uncertain quality (solderability class 4).

## Acknowledgment

The work has been carried out within research project “Improving the reliability of lead-free soldered joints in electronic packages,” No. WND-POIG.01.03.01-00-103/09, financed by the EC structural funds and the Ministry of Science and Higher Education of Poland.

## Open Access

This article is distributed under the terms of the Creative Commons Attribution License which permits any use, distribution, and reproduction in any medium, provided the original author(s) and the source are credited.

## References

1. J. Zhao, L. Qi, and X. Wang, Influence of Bi on Microstructures Evolution and Mechanical Properties in Sn-Ag-Cu Lead-Free Solder, *J. Alloys Compd.*, 2004, **375**(1-2), p 196–201
2. F. Zhu, H. Zhang, R. Guan, and S. Liu, Effects of Temperature and Strain Rate on Mechanical Property of Sn96.5Ag3Cu0.5, *J. Alloys Compd.*, 2007, **438**, p 100–106
3. K. Kanlayasiri, M. Mongkolwongrojn, and T. Ariga, Influence of Indium Addition on Characteristics of Sn-0.3Ag-0.7Cu Solder Alloy, *J. Alloys Compd.*, 2009, **485**(1-2), p 225–230
4. I. Anderson, Development of Sn-Ag-Cu and Sn-Ag-Cu-X Alloys for Pb-Free Electronic Solder Applications, *J. Mater. Sci. Mater. Electron.*, 2007, **18**, p 55–76
5. K. Suganuma, Advances in Lead-Free Electronics Soldering, *Curr. Opin. Solid State Mater. Sci.*, 2001, **5**, p 55–64
6. H.T. Ma and J.C. Suhling, A Review of Mechanical Properties of Lead-Free Solders for Electronic Packaging, *J. Mater. Sci.*, 2009, **44**(5), p 1141–1158
7. M. Abtey and G. Selvaduray, Lead-Free Solders in Microelectronics, *Mater. Sci. Eng.*, 2000, **R27**, p 95–141

8. H.Y. Chang, S.W. Chen, D.S.H. Wong, and H.F. Hsu, Determination of Reactive Wetting Properties of Sn, Sn-Cu, Sn-Ag, and Sn-Pb Alloys Using a Wetting Balance Technique, *J. Mater. Res.*, 2003, **18**, p 1420–1428
9. H.H. Manko, *Solders and Soldering*, 3rd ed., McGraw-Hill Inc, New York, 1992, p 1–153
10. N. Sobczak, A. Kudyba, R. Nowak, W. Radziwill, and K. Pietrzak, Factors affecting wettability and bond strength of solder joint couples, *Pure. Appl. Chem.*, 2007, **79**(10), p 1755
11. S. Vaynman and M.E. Fine, Development of Fluxes for Lead free Solders Containing Zinc, *Scripta Mater.*, 1999, **41**(12), p 1269–1271
12. J. Shen and Y.C. Chan, Effect of Metal/Ceramic Nanoparticle-Doped Fluxes on the Wettability Between Sn-Ag-Cu Solder and a Cu Layer, *J. Alloys Compd.*, 2009, **477**, p 909–914
13. K. Narayan Prabhu, R. Bali, and R. Ranjan, Effect of Substrate Surface Texture and Flux Coating on the Evolution of Microstructure During Solidification of Lead Free Sn-3.5Ag Solder Alloy, *Mater. Des.*, 2004, **25**, p 447–449
14. V.H. Lopez and A.R. Kennedy, Flux-Assisted Wetting and Spreading of Al on TiC, *J. Colloid Interface Sci.*, 2006, **298**(1), p 356–362
15. D.E. Peebles, H.C. Peebles, and J.A. Ohlhausen, Kinetics of the Isothermal Spreading of Tin on the Air-Passivated Copper Surface in the Absence of Fluxing Agent, *Colloids Surf. A*, 1998, **144**, p 89–114
16. K.M. Martorano, M.A. Martorano, and S.D. Brandi, Optimal Conditions for Wetting Balance test, *J. Mater. Process. Technol.*, 2009, **209**, p 3089–3095
17. J.X. Wang, S.B. Xue, and Z.J. Han, Study on Wettability of Sn-Ag-Cu Solder and Mechanical Properties of Soldered Joints, *J. Mater. Eng.*, 2008, **9**, p 5–8
18. *ST88 Wettability Tester—User's Guide*, Metronelec, France, Issue 1, 2010
19. M.P. Groover, *Fundamentals of Modern Manufacturing: Materials Processes and Systems*, Wiley, New York, 2000, ISBN 978-0470-467002
20. R.J. Klein Wassink, *Soldering in Electronics*, 2nd ed., Electrochemical Publications Ltd., Bristol, 1994, ISBN 090115024X
21. K. Zeng and K.N. Tu, Six Cases of Reliability Study of Pb-Free Solder Joints in Electronic Packaging Technology, *Mater. Sci. Eng.*, 2002, **38**, p 55–105
22. L.C. Tsao, Evolution of Nano-Ag<sub>3</sub>Sn Particle Formation on Cu-Sn Intermetallic Compounds of Sn<sub>3.5</sub>Ag<sub>0.5</sub>Cu Composite Solder/Cu During Soldering, *J. Alloys Compd.*, 2011, **509**, p 2326–2333
23. Y.C. Lin, K.J. Wang, and J.G. Duh, Detailed Phase Evolution of a Phosphorous-Rich Layer and Formation of the Ni-Sn-P Compound in Sn-Ag-Cu/Electroplated Ni-P Solder Joints, *J. Electron. Mater.*, 2010, **39**, p 283–293
24. J. Wojewoda-Budka, Z. Huber, L. Litynska-Dobrzynska, N. Sobczak, and P. Zieba, Microstructure and Chemistry of the Solder/ENIG Interconnections, *Mater. Chem. Phys.*, 2012, doi: [org/10.1016/j.matchemphys.2013.01.035](https://doi.org/10.1016/j.matchemphys.2013.01.035)